Heliyon 9 (2023) e16810

Contents lists available at ScienceDirect

Heliyon

journal homepage: www.cell.com/heliyon

Age-related morphometrics of normal adrenal glands based on deep learning-aided segmentation

Yuanchong Chen [a], Jiejin Yang [a], Yaofeng Zhang [b], Yumeng Sun [b], Xiaodong Zhang [a], Xiaoying Wang [a,*]

[a] Department of Radiology, Peking University First Hospital, Beijing, 100034, China
[b] Beijing Smart-imaging Technology Co. Ltd., Beijing, 100011, China

ARTICLE INFO

Keywords:
Adrenal gland
Deep learning
Morphometrics
Computed tomography

ABSTRACT

Objective.

This study aims to evaluate the morphometrics of normal adrenal glands in adult patients semiautomatically using a deep learning-based segmentation model.

Materials and Methods.

A total of 520 abdominal CT image series with normal findings, from January 1, 2016, to March 14, 2019, were retrospectively collected for the training of the adrenal segmentation model. Then, 1043 portal venous phase image series of inpatient contrast-enhanced abdominal CT examinations with normal adrenal glands were included for analysis and grouped by every 10-year gap. A 3D U-Net-based segmentation model was used to predict bilateral adrenal labels followed by manual modification of labels as appropriate. Quantitative parameters (volume, CT value, and diameters) of the bilateral adrenal glands were then analyzed.

Results.

In the study cohort aged 18–77 years old (554 males and 489 females), the left adrenal gland was significantly larger than the right adrenal gland [all patients, 2867.79 (2317.11–3499.89) mm^3 vs. 2452.84 (1983.50–2935.18) mm^3, $P < 0.001$]. Male patients showed a greater volume of bilateral adrenal glands than females in all age groups (all patients, left: 3237.83 ± 930.21 mm^3 vs. 2646.49 ± 766.42 mm^3, $P < 0.001$; right: 2731.69 ± 789.19 mm^3 vs. 2266.18 ± 632.97 mm^3, $P = 0.001$). Bilateral adrenal volume in male patients showed an increasing then decreasing trend as age increased that peaked at 38–47 years old (left: 3416.01 ± 886.21 mm^3, right: 2855.04 ± 774.57 mm^3).

Conclusions.

The semiautomated measurement revealed that the adrenal volume differs as age increases. Male patients aged 38–47 years old have a peaked adrenal volume.

1. Introduction

The adrenal gland plays a vital role in homeostasis and stress responses. The y-shaped glands are located superior to the kidney and are adjacent to the liver, gastric wall, and crus of the diaphragm [1]. Previous studies have shown that changes in adrenal

* Corresponding author. Department of Radiology, Peking University First Hospital No. 8 Xishiku St., Xicheng District, Beijing, 100034, China.
E-mail address: wangxiaoying@bjmu.edu.cn (X. Wang).

https://doi.org/10.1016/j.heliyon.2023.e16810
Received 16 March 2023; Received in revised form 21 May 2023; Accepted 29 May 2023
Available online 30 May 2023

morphometrics (i.e., shape, density, and volume) may represent adrenal functions to some extent [2].

Computed tomography (CT) is the modality of choice in diagnosing adrenal lesions [3,4]. Focal or diffuse abnormalities can be discovered on CT images, leading to the diagnosis of adrenal diseases. Changes in adrenal morphometrics may also reflect functional alterations and be relevant to some diseases [5–11], but these studies mostly remained qualitative. Previous studies have shown considerable effectiveness in diagnosing primary aldosteronism [12]. Volumetric assessment of adrenal glands on CT images remained qualitative in the conventional diagnosis workflow due to the complexity and time-consuming manual quantitative measuring process, and previous preliminary quantitative studies of adrenal volume have a limited sample size due to the same reasons [13,14]. Hence, adrenal functional abnormalities may be missed if the precise volume of the adrenal gland is not given. In the era of artificial intelligence, several networks were developed and refurbished in medical image processing [15–18], and the 3D U-Net is the classic and most used one for medical image segmentation [19,20]. Deep learning-based segmentation models of the spine, liver, kidney, pancreas, and prostate have been applied in CT and MR images and have achieved considerable efficacy [21–23]. An adrenal segmentation model based on a similar architecture can be developed and used for automatic measurements, such as density, volume, and diameters, aiding in the efficient and accurate quantitative description of the adrenal gland that has the potential to promote the diagnosis of adrenal diseases. Moreover, such a segmentation model laid the root for further adrenal classification and focal lesion segmentation. However, the irregularity and tiny shape of the adrenal gland make segmentation challenging [24,25].

Previous small-sample studies ($N < 150$) did not show the age-related distribution of adrenal volume [14,26–28]. These morphological studies did not utilize the semiautomated segmentation process based on deep learning. To date, the morphometrics of normal adrenal glands has not been studied in a relatively large sample. Recent deep learning-based studies mainly focused on the comparison between normal and abnormal adrenal glands [29,30]. The present study established a 3D U-Net [31]-based model for the automatic segmentation of adrenal glands in abdominal CT images and tried to discover the changes in morphometrics of normal adrenal glands in different age groups.

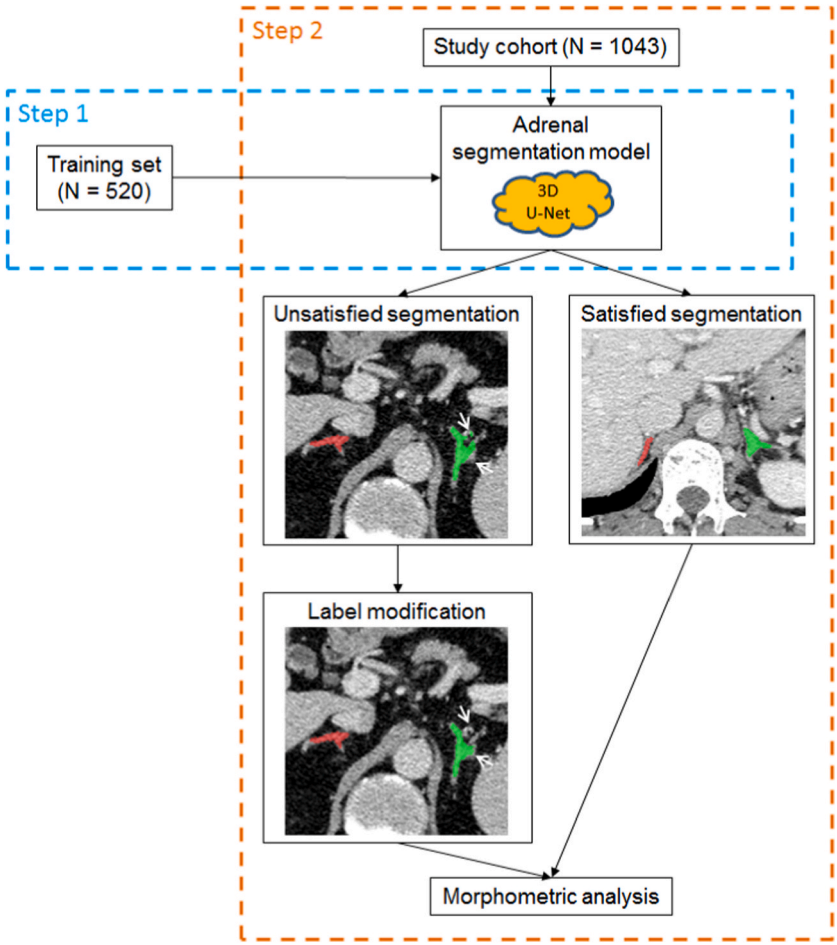

Fig. 1. Study flowchart. A 3D U-Net-based adrenal segmentation model was trained using the training set (N = 520). Images of the study cohort (N = 1043) underwent label prediction, and adrenal segmentation results were checked by an experienced radiologist. Unsatisfactory segmentation was modified accordingly (shown in white arrows) and then enrolled for morphometric analysis in combination with initially satisfied segmentation.

2. Materials and Methods

2.1. Patients

This retrospective study was approved by the institutional review board of Peking University First Hospital [No. 2019 (169)], with a waiver of informed consent.

2.2. Training set for a 3D U-Net segmentation model

Thin-slice reconstructed images (slice thickness 1 mm, 1.25 mm, and 1.5 mm) of patients who underwent abdominal CT scans (both non-contrast and multiphase contrast-enhanced) diagnosed with no obvious abnormalities in our center from January 1st, 2016 to March 14th, 2019 were retrospectively collected and transferred from PACS to the training platform. These images were acquired by GE Discovery CT750HD, GE LightSpeed VCT, Siemens SOMATOM Definition Flash, Philips Brilliance iCT 256, and Philips Brilliance 64. The exclusion criteria were as follows: 1) images could not be retrieved; 2) parts of adrenal glands were out of the scan range; 3) suspicious or existing adrenal lesions were found upon re-evaluation; 4) the patient was not in a supine position; and 5) poor image quality due to motion or metal artifacts. Finally, 434 accessions (520 thin-sliced series) were included. Left and right adrenal glands were labeled separately by a junior radiologist (with 2 years of experience) in each image series using ITK-SNAP v3.6.0 and checked by a senior radiologist (with 25 years of experience). Images were randomly allotted into a training set (left N = 419, right N = 413), validation set (left N = 53, right N = 55), and test set (left N = 48, right N = 52) to establish the 3D U-Net-based adrenal segmentation model (Fig. 1).

2.3. Study cohort for volume measurement

Portal venous phase images of inpatient abdominal contrast-enhanced CT scans in our center were collected from March 15th, 2019, to March 31st, 2022. Patients aged from 18 years to 77 years were grouped every 10 years. Image series were included in each

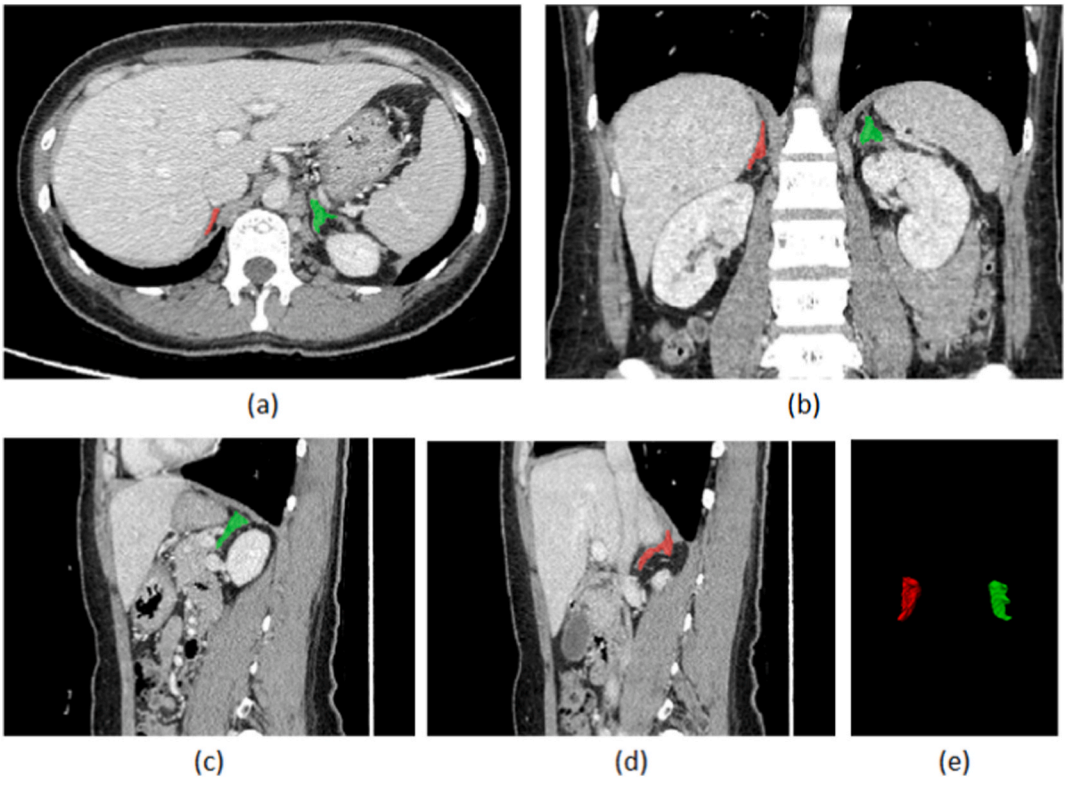

Fig. 2. Labeled adrenal gland on portal venous phase CT image. A 38-year-old female with normal bilateral adrenal glands underwent contrast-enhanced CT scan that showed in multiplanar reconstruction of axial (a), coronal (b), and sagittal (c, d) views. A 3D view of the bilateral adrenal glands is shown in (e). Red label, right adrenal gland; green label, left adrenal gland. The quantitative parameters were as follows: right adrenal gland: volume 2762 mm^3, CT value 62 HU, 3D diameters 12.9 mm × 34.5 mm × 40.3 mm; left volume 2375 mm^3, CT value 62 HU, 3D diameters 14.9 mm × 20.2 mm × 36.7 mm. (For interpretation of the references to colour in this figure legend, the reader is referred to the Web version of this article.)

Table 1
Quantitative parameters of bilateral adrenal glands in different age groups.

		All	18-27					28-37						38-47						48-57						58-67						68-77					
			All	Male	Female	Statistical value	P value	All	Male	Female	Statistical value	P value		All	Male	Female	Statistical value	P value		All	Male	Female	Statistical value	P value		All	Male	Female	Statistical value	P value		All	Male	Female	Statistical value	P value	
Count		1043 (100.00%)	144 (13.81%)	61 (42.36%)	83 (57.64%)			170 (16.30%)	81 (47.65%)	89 (52.35%)				168 (16.11%)	95 (56.55%)	73 (43.45%)				185 (17.74%)	108 (58.38%)	77 (41.62%)				188 (18.02%)	103 (54.79%)	85 (45.21%)				188 (18.02%)	106 (56.38%)	82 (43.62%)			
Age		50.00 (34.00 - 64.00)	24.00 (21.00 - 26.00)	22.67 ± 3.02 (21.91 - 23.43)	24.00 (21.00 - 26.00)	2101.00	0.040	33.00 (30.00 - 35.00)	33.00 (30.00 - 35.00)	32.70 ± 2.81 (32.11 - 33.28)	3482.50	0.352		44.00 (41.00 - 46.00)	44.00 (40.50 - 46.00)	43.25 ± 2.95 (42.57 - 43.92)	3465.50	0.498		54.00 (50.00 - 56.00)	54.00 (50.00 - 55.50)	54.00 (50.00 - 56.00)	3991.50	0.320		63.00 (60.00 - 65.00)	62.62 ± 2.62 (62.12 - 63.13)	62.56 ± 2.78 (61.97 - 63.16)	4340.50	0.461		72.00 (69.00 - 74.00)	71.81 ± 2.66 (71.31 - 72.32)	72.23 ± 3.00 (71.58 - 72.88)	4008.00	0.179	
Volume/mm^3	Right	2452.84 (1983.50 - 2935.18)	2055.59 (1683.95 - 2550.47)	2438.19 ± 784.06 (2241.42 - 2634.95)	2057.07 ± 739.21 (1898.04 - 2216.10)	1721.00	0.001	2457.31 ± 752.14 (2344.25 - 2570.38)	2713.37 ± 836.54 (2531.19 - 2895.55)	2224.27 ± 574.20 (2104.98 - 2343.57)	4.38	0.000		2591.70 ± 742.40 (2479.44 - 2703.97)	2855.04 ± 774.57 (2699.28 - 3010.80)	2249.01 ± 529.13 (2127.63 - 2370.39)	5.98	0.000		2567.72 ± 705.94 (2466.00 - 2669.45)	2786.80 ± 708.96 (2653.09 - 2920.51)	2260.44 ± 574.99 (2132.01 - 2388.87)	5.53	0.000		2635.71 ± 772.39 (2525.30 - 2746.12)	2836.99 ± 820.89 (2678.46 - 2995.52)	2391.80 ± 627.97 (2258.30 - 2525.30)	4.08	0.000		2544.49 ± 723.99 (2441.00 - 2647.98)	2645.58 ± 759.76 (2500.94 - 2790.22)	2413.81 ± 652.12 (2272.66 - 2554.96)	2.19	0.030	
	Left	2867.79 (2317.11 - 3499.89)	2459.58 (2008.72 - 3146.97)	3053.41 ± 1190.84 (2754.56 - 3352.25)	2417.61 ± 759.30 (2254.26 - 2580.97)	1714.00	0.000	2843.83 ± 937.20 (2702.95 - 2984.72)	3068.81 ± 981.16 (2855.14 - 3282.49)	2639.07 ± 844.75 (2463.57 - 2814.58)	3.05	0.003		3075.62 ± 890.33 (2940.99 - 3210.26)	3416.01 ± 886.21 (3237.80 - 3594.22)	2632.66 ± 674.69 (2477.89 - 2787.44)	6.47	0.000		3005.43 ± 880.05 (2878.61 - 3132.24)	3274.21 ± 868.46 (3110.41 - 3438.00)	2628.43 ± 747.97 (2461.36 - 2795.50)	5.25	0.000		3096.16 ± 876.06 (2970.93 - 3221.39)	3377.61 ± 904.78 (3202.88 - 3552.35)	2755.11 ± 702.28 (2605.81 - 2904.41)	5.16	0.000		2993.26 ± 797.14 (2879.31 - 3107.21)	3140.51 ± 776.70 (2992.65 - 3288.38)	2802.91 ± 782.78 (2633.48 - 2972.33)	2.93	0.004	
Average CT value/HU	Right	61.18 ± 13.91 (60.33 - 62.02)	66.85 ± 14.43 (64.49 - 69.21)	60.83 ± 13.65 (57.40 - 64.25)	71.28 ± 13.35 (68.41 - 74.15)	-4.57	0.000	62.99 ± 13.17 (61.01 - 64.97)	55.54 ± 10.99 (53.15 - 57.94)	69.77 ± 11.19 (67.45 - 72.09)	-8.30	0.000		61.27 ± 14.29 (59.11 - 63.43)	55.08 ± 11.64 (52.74 - 57.42)	69.31 ± 13.37 (66.25 - 72.38)	-7.32	0.000		57.59 ± 12.12 (55.85 - 59.34)	55.07 ± 11.41 (52.92 - 57.22)	61.13 ± 12.20 (58.41 - 63.85)	-3.44	0.001		59.26 ± 14.97 (57.12 - 61.40)	52.80 ± 11.41 (50.59 - 55.00)	67.08 ± 15.04 (63.89 - 70.28)	-7.36	0.000		60.56 ± 12.73 (58.74 - 62.38)	56.63 ± 10.82 (54.57 - 58.69)	65.64 ± 13.22 (62.78 - 68.50)	-4.98	0.000	
	Left	64.24 ± 16.28 (63.25 - 65.22)	73.38 ± 18.55 (70.35 - 76.41)	65.26 ± 16.38 (61.15 - 69.37)	79.35 ± 17.76 (75.53 - 83.17)	-4.83	0.000	66.19 ± 16.33 (63.73 - 68.64)	57.44 ± 14.45 (54.29 - 60.59)	74.15 ± 13.66 (71.31 - 76.98)	-7.70	0.000		63.82 ± 16.30 (61.35 - 66.28)	57.05 ± 12.72 (54.49 - 59.60)	72.63 ± 16.25 (68.90 - 76.35)	-6.71	0.000		59.30 ± 13.12 (57.41 - 61.19)	56.15 ± 11.86 (53.92 - 58.39)	63.71 ± 13.53 (60.69 - 66.73)	-4.00	0.000		61.52 ± 16.28 (59.19 - 63.84)	55.38 ± 13.72 (52.73 - 58.03)	68.95 ± 16.03 (65.54 - 72.36)	-6.22	0.000		63.41 ± 13.93 (61.42 - 65.41)	59.50 ± 12.15 (57.18 - 61.81)	68.48 ± 14.43 (65.36 - 71.61)	-4.61	0.000	
Diameters/mm	Right x	18.87 (16.34 - 21.81)	17.07 ± 3.64 (16.47 - 17.66)	18.25 ± 3.73 (17.31 - 19.18)	16.20 ± 3.32 (15.49 - 16.92)	3.44	0.001	18.24 ± 4.20 (17.61 - 18.87)	20.20 ± 4.47 (19.23 - 21.18)	16.45 ± 2.98 (15.83 - 17.07)	6.33	0.000		19.68 ± 4.39 (19.01 - 20.34)	21.30 ± 4.18 (20.46 - 22.14)	17.56 ± 3.71 (16.71 - 18.41)	6.00	0.000		19.05 ± 3.62 (16.93 - 21.88)	20.79 (20.11 - 21.47)	17.53 (15.36 - 19.82)	2195.00	0.000		19.26 ± 4.27 (17.22 - 22.93)	19.79 ± 4.34 (17.61 - 23.67)	19.22 ± 3.36 (18.51 - 19.94)	3544.00	0.012		20.31 ± 4.27 (19.70 - 20.92)	20.91 ± 4.34 (20.08 - 21.74)	19.54 ± 4.05 (18.66 - 20.41)	2.20	0.029	
	Right y	34.38 (30.07 - 39.34)	32.83 (28.95 - 37.20)	35.21 ± 8.12 (33.17 - 37.25)	32.04 (28.62 - 35.27)	1918.00	0.000	33.29 (29.43 - 37.53)	35.60 (31.45 - 39.55)	31.70 (28.88 - 34.86)	2382.00	0.000		34.59 ± 6.82 (30.75 - 38.63)	36.18 ± 6.82 (34.81 - 37.55)	32.83 (28.88 - 37.40)	2710.00	0.008		36.34 (31.99 - 42.64)	36.83 (32.27 - 42.55)	35.96 (31.02 - 44.18)	3892.50	0.230		35.86 (30.82 - 42.11)	37.96 (32.77 - 43.95)	32.83 (29.44 - 38.07)	3227.00	0.001		33.68 ± 9.73 (29.56 - 38.89)	36.35 ± 6.64 (34.50 - 38.20)	32.64 (28.71 - 36.91)	3574.50	0.019	
	Right z	35.00 (31.00 - 39.00)	36.06 ± 7.10 (34.90 - 37.22)	37.07 ± 6.90 (35.34 - 38.80)	35.32 ± 7.15 (33.78 - 36.85)	1.47	0.144	36.84 ± 5.76 (35.97 - 37.71)	37.59 ± 6.04 (36.27 - 38.90)	35.34 ± 5.40 (35.04 - 37.28)	1.61	0.109		36.45 ± 5.92 (35.55 - 37.34)	37.29 ± 6.04 (36.08 - 38.51)	35.34 ± 5.57 (34.06 - 36.62)	2.13	0.034		35.58 ± 5.60 (34.77 - 36.38)	35.56 ± 4.96 (34.62 - 36.50)	35.60 ± 6.38 (34.17 - 37.02)	-0.04	0.968		35.00 (30.00 - 38.00)	35.00 (30.53 - 38.00)	34.63 ± 6.00 (33.36 - 35.91)	4342.50	0.463		33.42 ± 6.62 (32.47 - 34.36)	33.95 ± 6.75 (32.66 - 35.23)	32.73 ± 6.38 (31.35 - 34.11)	1.25	0.213	
	Left x	19.64 (16.46 - 22.76)	15.94 (14.04 - 19.51)	19.14 ± 5.56 (17.75 - 20.53)	15.29 (13.46 - 16.98)	1624.50	0.000	17.94 (15.04 - 20.84)	19.86 (16.68 - 23.03)	16.62 ± 3.48 (15.90 - 17.34)	1965.00	0.000		20.56 ± 5.58 (19.72 - 21.40)	22.46 ± 5.13 (21.42 - 23.49)	18.10 ± 5.15 (16.91 - 19.28)	5.42	0.000		20.00 (17.09 - 22.95)	21.09 ± 5.07 (18.44 - 23.71)	19.23 ± 5.07 (18.10 - 20.36)	2651.00	0.000		21.18 ± 4.28 (20.57 - 21.79)	22.15 ± 3.85 (21.40 - 22.89)	20.01 ± 4.49 (19.06 - 20.97)	3.49	0.001		20.50 ± 4.40 (18.45 - 23.66)	21.83 ± 4.40 (18.86 - 23.94)	19.55 ± 4.46 (17.46 - 21.46)	3373.50	0.000	
	Left y	34.05 ± 7.53 (33.59 - 34.50)	32.18 ± 7.32 (30.98 - 33.37)	35.19 ± 7.95 (33.19 - 37.18)	29.97 ± 5.91 (28.70 - 31.24)	4.29	0.000	33.05 ± 6.25 (32.11 - 33.99)	34.83 ± 6.59 (33.39 - 36.26)	31.43 ± 5.45 (30.30 - 32.56)	3.66	0.000		34.15 ± 7.47 (33.02 - 35.28)	36.66 ± 7.10 (35.23 - 38.09)	30.87 ± 6.62 (29.35 - 32.39)	5.36	0.000		35.01 ± 7.99 (33.86 - 36.16)	37.45 ± 7.91 (35.96 - 38.94)	31.59 ± 6.74 (30.08 - 33.10)	5.25	0.000		34.62 ± 8.04 (33.47 - 35.77)	37.63 ± 7.83 (36.12 - 39.14)	30.97 ± 6.68 (29.55 - 32.39)	6.17	0.000		34.77 ± 7.43 (33.70 - 35.83)	37.04 ± 7.43 (35.63 - 38.46)	31.82 ± 6.31 (30.46 - 33.19)	5.07	0.000	
	Left z	37.00 (32.00 - 42.00)	38.00 (33.50 - 42.00)	39.41 ± 7.50 (37.53 - 41.30)	38.23 ± 8.98 (36.30 - 40.16)	2319.50	0.196	38.45 ± 8.01 (37.25 - 39.66)	39.28 ± 8.96 (37.33 - 41.23)	37.70 ± 6.95 (36.26 - 39.14)	1.29	0.200		38.33 ± 7.65 (37.17 - 39.48)	39.00 ± 7.85 (37.42 - 40.58)	37.45 ± 7.30 (35.78 - 39.13)	1.30	0.196		37.02 ± 8.09 (35.85 - 38.18)	37.11 ± 8.08 (35.59 - 38.64)	36.89 ± 8.10 (35.08 - 38.70)	0.19	0.852		36.54 ± 8.15 (35.38 - 37.71)	36.42 ± 7.97 (34.88 - 37.96)	36.70 ± 8.36 (34.92 - 38.47)	-0.23	0.817		34.82 ± 7.15 (33.80 - 35.84)	34.85 ± 7.26 (33.47 - 36.24)	34.78 ± 7.00 (33.27 - 36.30)	0.07	0.947	

Data are described as mean ± standard deviation (95% confidence interval) or median (interquartile range), depending on normality. The statistical value and p value demonstrate the comparison between male and female patients in each age group.

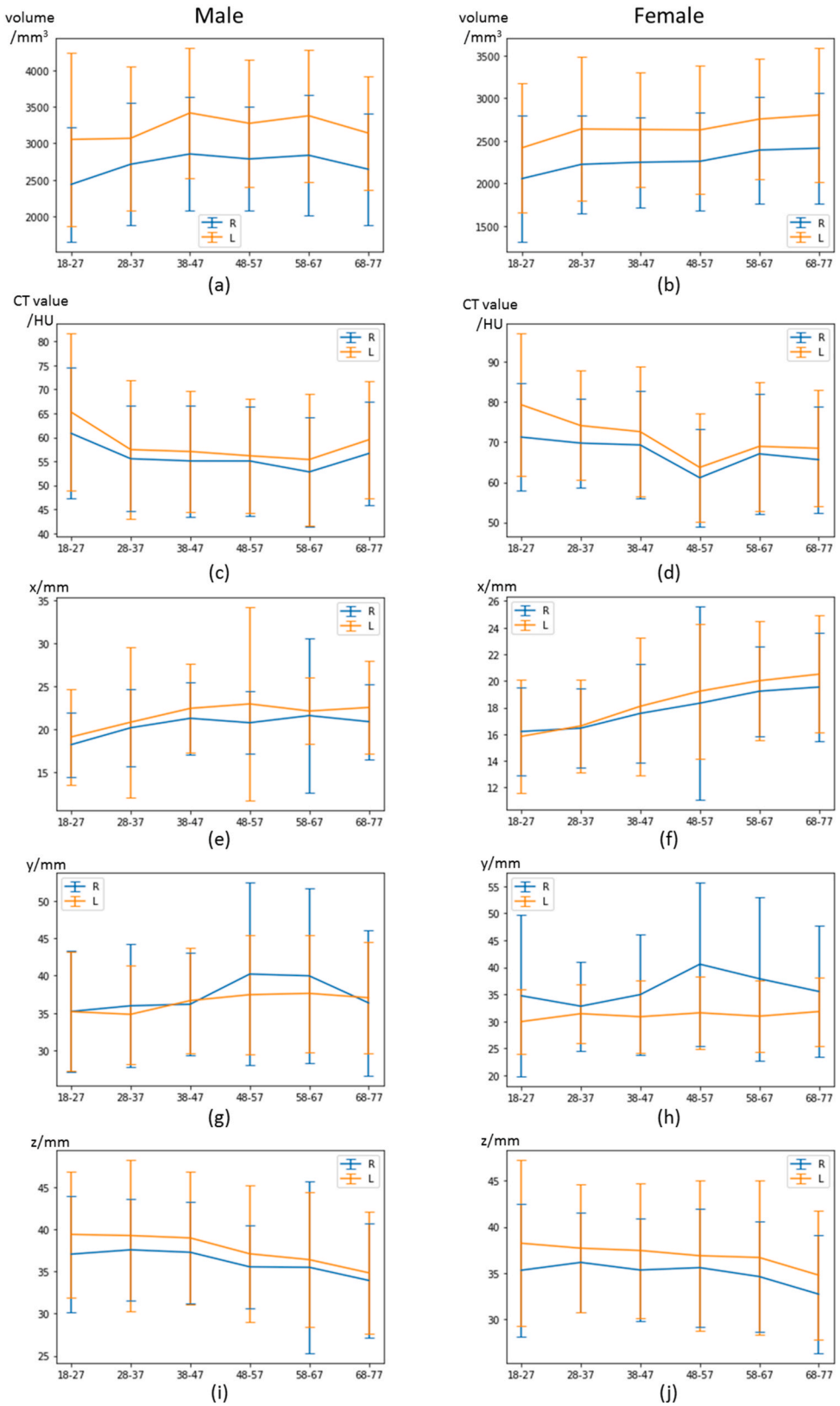

Fig. 3. Changes in volume (a, b), CT value (portal venous phase) (c, d), and diameters (e–i) in adrenal glands in different age groups. Male (a, c, e, g, i) and female (b, d, f, h, j) patients are shown.

age group consecutively until reaching 200 series in each group. These images were acquired by GE Discovery CT750HD, GE Light-Speed VCT, Siemens SOMATOM Definition Flash, and Philips Brilliance iCT 256. The inclusion criteria were as follows: 1) imaging findings containing "normal bilateral adrenal glands" and 2) no adrenal diseases diagnosed upon discharge based on comprehensive physical examinations and laboratory tests, including complete biochemical profiles of blood and urine. The exclusion criteria were those of the training set, plus: 1) CT peritoneography or enterography with positive contrast agent; 2) severe deformity (e.g., scoliosis); and 3) postoperative changes that affected adjacent structures of the adrenal gland. 1200 series were finally included. The earliest image series of patients who had multiple examinations was kept, and follow-up examinations were then excluded. Finally, 1043 series were enrolled for analysis.

2.4. Model training

This study was based on a 3D U-Net architecture equipped with Nvidia Tesla P100 16G (Nvidia Corporation, Santa Clara, CA) GPU and PyTorch v1.7.1 + cu110 (https://pytorch.org/). The model inputs CT images and outputs bilateral adrenal volume, average CT values, and three-dimensional diameters. Image preprocessing included window adjustment (center 30 HU, width 300 HU), resizing to 128 px × 192 px × 256 px, and image augmentation by rotating, sheering, noise injection, denoising, etc. The training parameters were batch size 6, learning rate 0.0001, and epoch 400. Details were shown in the Supplementary Materials.

2.5. Quantitative measurements

Image series in the study cohort underwent autolabeling by the adrenal segmentation model. These bilateral adrenal labels were checked by a junior radiologist and a senior radiologist together, and unsatisfied labels were modified manually. Necessary manual modification of labels was performed to ensure that the labeled area (as a region of interest [ROI]) contained the left/right adrenal gland only (Fig. 2 (a)-(e)), and adjacent structures, such as the gastric wall, kidney, or liver, were not covered. Labels that exceeded or missed 5% of ipsilateral adrenal volume were also modified. The volume, average CT values, and three-dimensional diameters of the ROIs were measured.

2.6. Statistical analysis

Statistical analysis was performed using Python 3.7.6 (Python, The Netherlands) with scipy 1.4.1, statsmodels 0.11.0, and sklearn 0.22.1 unless specified. All analyses were 2-sided, and the statistical significance was set at $P < 0.05$. Data normality was determined by the Kolmogorov–Smirnov test. Continuous variables in univariate analysis were compared using Student's t-test and the Mann–Whitney *U* test, as appropriate.

3. Results

As shown in Table 1, the average age of all patients (N = 1043) was 50.00 (37.00–64.00) years (median [interquartile range, IQR]), and the average adrenal volume was 2452.84 (1983.50–2935.18) mm^3 on the right and 2867.79 (2317.11–3499.89) mm^3 on the left in the study cohort. The volume of the left adrenal gland was greater than that of the contralateral adrenal gland regardless of age or sex ($P < 0.001$). The adrenal volume of male patients was significantly larger than that of female patients bilaterally ($P < 0.05$) among all age groups. Adrenal volume differed in different age groups. It showed an increasing then decreasing trend of bilateral adrenal volume as age increased in male patients who peaked at 38–47 years old (right 2591.70 ± 742.40 mm^3 (mean ± standard deviation [SD]), left 3075.62 ± 890.33 mm^3; Fig. 3(a)(b)). The CT values of the right and left adrenal glands in portal venous phase in the study cohort were 61.18 ± 13.91 HU and 64.24 ± 16.28 HU, respectively, with a significant difference between males and females ($P < 0.001$) in all age groups. Enhanced CT values of adrenal glands showed a decreasing then increasing trend as age increased (Fig. 3(c)(d)). The 3D diameters (x × y × z) of the adrenal glands were 18.87 (16.34–21.81) mm × 34.38 (30.07–39.34) mm × 35.00 (31.00–39.00) mm (right) and 19.64 (16.46–22.76) mm × 34.05 ± 7.53 mm × 37.00 (32.00–42.00) mm (left) in all included patients (Fig. 3 (e)–(j)).

4. Discussion

The quantitative parameters of organs in medical imaging play an important role in disease diagnosis. A reliable segmentation model enables automated and standardized morphometric measurement of organs and will undoubtedly improve the efficiency and precision of diagnosis. Currently, segmentation models of some solitary organs have been used for target volume delineation in radiotherapy planning. Segmenting the adrenal gland and measuring adrenal volume on CT images can reflect functional abnormalities of the adrenal gland represented by hypertrophy or atrophy [32,33].

The segmentation model used in this study can be applied to large-volume samples in the automatic measurement of adrenal glands in thin-slice CT images. Portal vein phase images of contrast-enhanced CT examinations were used because of the relatively good contrast between organs and blood vessels. In the study cohort, the adrenal volume showed an increasing then decreasing trend in male patients, which was compatible with previous anatomical studies on adrenal weight [34]. Adrenal volume peaks in 38- to 47-year-olds, indicating the period of maximal adrenal function [35,36]. However, the interesting pattern of adrenal CT values (portal venous phase) that bottomed at 48- to 57-year-olds cannot be explained by current literature. Further larger sample studies with controlled contrast-enhancing protocol and relative enhancing ratio calculation are needed to interpret such a pattern. Although the left-to-right

ratio of adrenal volume was reportedly useful in identifying unilateral primary aldosteronism [37], the physiologic left-to-right adrenal difference has not yet been described and explained.

The present study tried to discover age-related distribution as well as provide a reference range of normal adrenal volume that may help further morphological and functional evaluations of the adrenal gland. Abnormality in adrenal volume may indicate disturbances of the hypothalamic–pituitary–adrenal axis (HPA axis). Adrenal hypofunction caused by tuberculosis, autoimmune diseases, contralateral functioning adenoma, or a large amount of exogenous glucocorticoids may lower the adrenal volume, while abnormally enlarged adrenal glands usually indicate hypersecretion or ectopic secretion of upstream hormones (i.e., adrenocorticotropic hormone [ACTH]) caused by underlying tumors [6,7,38–41]. Other studies also showed the relation between changes in quantitative adrenal parameters and obesity [5], depression [42,43], type 2 diabetes mellitus [10,44], polycystic ovary syndrome (PCOS) [9], and obstructive sleep apnea-hypopnea syndrome (OSAHS) [8]. However, there is no exact mechanism explaining adrenal volumes beyond normal variation despite obvious adrenal diseases. Moreover, the follow-up examination of adrenal volume in patients using glucocorticoids can help with dose adjustment individually, preventing adrenal crisis, especially during the tapering-off period. The demand for adrenal functions increases under stress, such as septic shock [45], and failure of adrenal response may indicate an unfavorable prognosis [46] despite adrenal response to acute stress (e.g., cardiac arrest) may not be relevant to adrenal volume [47]. Quantitative adrenal parameters can predict treatment response in such patients and guide further management strategies thereafter.

The present study has several strengths. The semiautomated process of adrenal measurement and relatively large sample size of the present study stand out from previous studies [13,14] ($N < 150$). This evaluation method would enable efficient result-obtaining after the expansion of sample size in the future that has the potential to generate the reference range of adrenal volume which is not currently known, as well as investigating the relationship between adrenal functions and its morphometrics. Moreover, parameters other than volume (i.e., enhanced CT values, diameters of adrenal glands, and thickness of adrenal limbs) that may also contribute to physiological or abnormal functional predictions were included for primary analysis. Enhanced CT values of normal adrenal glands have not been reported and analyzed previously. Complex analyses on the relative enhancing ratio (which has been used in focal lesions [48]) and adrenal-to-body metrics in further studies are needed to confirm this.

There are several limitations to this observational study. Only inpatient data without long-term follow-up were included in this study. Whether other diseases will affect adrenal volume remains unclear, although they do not have adrenal diseases. Multicenter and healthy population-based studies are needed for further investigation of age-related distribution and setting of the reference range of adrenal volume. The relationship between adrenal morphometrics and body mass index or adrenal function profile based on laboratory tests is to be discovered as well. The present study only focused on adrenal situations at a certain time. It cannot be determined whether any of the included patients had underlying adrenal diseases that were subclinical in the study period and became symptomatic later on. A long-term cohort study is needed to exclude those patients as much as possible, as well as to discover the relationship between adrenal morphometrics and subclinical diseases. Nevertheless, changes in adrenal morphometrics in the same patient may represent the physiological aging process more precisely than the present cross-sectional study. Young ($<$18 years old) and elderly patients ($\geq$78 years old) were not included in the present study. Studies including such objects are still needed to understand the complete picture of adrenal volumetric changes.

5. Conclusion

A deep learning-based segmentation model can be used in adrenal volumetric measurement. With the help of such model, it revealed that the volume of the adrenal gland varies in different age groups. Male patients have a larger adrenal volume that peaks in middle age.

Funding

None.

Authors' contributions

YC, XZ, and XW conceived and designed the experiments; YC, JY, YZ, and YS performed the experiments; YC, XZ, and XW analyzed and interpreted the data; YC, JY, YZ, YS, XZ, and XW contributed reagents, materials, analysis tools or data; YC and XW wrote the paper. All authors read and approved the final manuscript.

Availability of data and material

The datasets used and analyzed during the current study are available from the corresponding author on reasonable request.

Declaration of competing interest

The authors declare that they have no known competing financial interests or personal relationships that could have appeared to influence the work reported in this paper.

Acknowledgements

The authors acknowledge the entire staff of the Department of Radiology, Peking University First Hospital as well as the technical support team of Beijing Smart-imaging Technology Co. Ltd.

Appendix A. Supplementary data

Supplementary data to this article can be found online at https://doi.org/10.1016/j.heliyon.2023.e16810.

References

[1] G. Lal, Q.Y. Duh, Laparoscopic adrenalectomy-indications and technique, Surg. Oncol. 12 (2003) 105–123.
[2] P.T. Johnson, K.M. Horton, E.K. Fishman, Adrenal mass imaging with multidetector CT: pathologic conditions, pearls, and pitfalls, Radiographics 29 (2009) 1333–1351.
[3] C. Yalniz, A.C. Morani, S.G. Waguespack, K.M. Elsayes, Imaging of adrenal-related endocrine disorders, Radiol. Clin. 58 (2020) 1099–1113.
[4] E. Kebebew, Adrenal incidentaloma, N. Engl. J. Med. 384 (2021) 1542–1551.
[5] F. Liu, Y. Chen, W. Xie, et al., Obesity might persistently increase adrenal gland volume: a preliminary study, Obes. Surg. 30 (2020) 3503–3507.
[6] M.S. Velema, L. Canu, T. Dekkers, et al., Volumetric evaluation of CT images of adrenal glands in primary aldosteronism, J. Endocrinol. Invest. 44 (2021) 2359–2366.
[7] R. Wurth, A. Tirosh, C.D.C. Kamilaris, et al., Volumetric modeling of adrenal gland size in primary bilateral macronodular adrenocortical hyperplasia, J. Endocr. Soc. 5 (2021), bvaa162.
[8] T. Minami, R. Tachikawa, T. Matsumoto, et al., Adrenal gland size in obstructive sleep apnea: morphological assessment of hypothalamic pituitary adrenal axis activity, PLoS One 14 (2019), e0222592.
[9] E. Gourgari, M. Lodish, M. Keil, et al., Bilateral adrenal hyperplasia as a possible mechanism for hyperandrogenism in women with polycystic ovary syndrome, J. Clin. Endocrinol. Metab. 101 (2016) 3353–3360.
[10] A.F. Godoy-Matos, A.R. Vieira, R.O. Moreira, et al., The potential role of increased adrenal volume in the pathophysiology of obesity-related type 2 diabetes, J. Endocrinol. Invest. 29 (2006) 159–163.
[11] C.B. Nemeroff, K.R. Krishnan, D. Reed, R. Leder, C. Beam, N.R. Dunnick, Adrenal gland enlargement in major depression. A computed tomographic study, Arch. Gen. Psychiatr. 49 (1992) 384–387.
[12] N.R. Dunnick, G.S. Leight Jr., M.A. Roubidoux, R.A. Leder, E. Paulson, L. Kurylo, CT in the diagnosis of primary aldosteronism: sensitivity in 29 patients, AJR Am. J. Roentgenol. 160 (1993) 321–324.
[13] J.M. Vincent, I.D. Morrison, P. Armstrong, R.H. Reznek, The size of normal adrenal glands on computed tomography, Clin. Radiol. 49 (1994) 453–455.
[14] X. Wang, Z.Y. Jin, H.D. Xue, et al., Evaluation of normal adrenal gland volume by 64-slice CT, Chin. Med. Sci. J. 27 (2013) 220–224.
[15] Y. Horai, M. Mizukawa, H. Nishina, et al., Quantification of histopathological findings using a novel image analysis platform, J. Toxicol. Pathol. 32 (2019) 319–327.
[16] A. Lagree, M. Mohebpour, N. Meti, et al., A review and comparison of breast tumor cell nuclei segmentation performances using deep convolutional neural networks, Sci. Rep. 11 (2021) 8025.
[17] M.M. Hossain, M.M. Hasan, M.A. Rahim, et al., Particle swarm optimized fuzzy CNN with quantitative feature fusion for ultrasound image quality identification, IEEE J. Transl. Eng. Health Med. (2022) 10.
[18] T.R. Mim, M. Amatullah, S. Afreen, et al., GRU-INC: an inception-attention based approach using GRU for human activity recognition, Expert Syst. Appl. (2023) 216.
[19] G.T. Du, X. Cao, J.M. Liang, X.L. Chen, Y.H. Zhan, Medical image segmentation based on U-net: a review, J. Imag. Sci. Technol. (2020) 64.
[20] N. Siddique, S. Paheding, C.P. Elkin, V. Devabhaktuni, U-net and its variants for medical image segmentation: a review of theory and applications, IEEE Access 9 (2021) 82031–82057.
[21] Y. Zhu, R. Wei, G. Gao, et al., Fully automatic segmentation on prostate MR images based on cascaded fully convolution network, J. Magn. Reson. Imag. 49 (2019) 1149–1156.
[22] X. Wei, X. Chen, C. Lai, Y. Zhu, H. Yang, Y. Du, Automatic liver segmentation in CT images with enhanced gan and mask region-based CNN architectures, BioMed Res. Int. 2021 (2021), 9956983.
[23] J. Cai, X. Guo, K. Wang, et al., Automatic Quantitative Evaluation of Normal Pancreas Based on Deep Learning in a Chinese Adult Population, Abdom Radiol, NY, 2022.
[24] G. Zhang, Z. Li, An adrenal segmentation model based on shape associating level set in sequence of CT images, J. Sign. Process. Syst. 91 (2019) 1169–1177.
[25] G. Luo, Q. Yang, T. Chen, T. Zheng, W. Xie, H. Sun, An optimized two-stage cascaded deep neural network for adrenal segmentation on CT images, Comput. Biol. Med. 136 (2021), 104749.
[26] B. Ludescher, A. Najib, S. Baar, et al., Gender specific correlations of adrenal gland size and body fat distribution: a whole body MRI study, Horm. Metab. Res. 39 (2007) 515–518.
[27] A. Mouritsen, M.L. Johansen, C. Wohlfahrt-Veje, et al., Determination of adrenal volume by MRI in healthy children: associations with age, body size, pubertal stage and serum levels of adrenal androgens, Clin. Endocrinol. 81 (2014) 183–189.
[28] J. Schneller, M. Reiser, F. Beuschlein, et al., Linear and volumetric evaluation of the adrenal gland-MDCT-based measurements of the adrenals, Acad. Radiol. 21 (2014) 1465–1474.
[29] T.M. Kim, S.J. Choi, J.Y. Ko, et al., Fully automatic volume measurement of the adrenal gland on CT using deep learning to classify adrenal hyperplasia, Eur. Radiol. 33 (2023) 4292–4302.
[30] C. Robinson-Weiss, J. Patel, B.C. Bizzo, et al., Machine learning for adrenal gland segmentation and classification of normal and adrenal masses at CT, Radiology 306 (2023), e220101.
[31] O. Ronneberger, P. Fischer, T. Brox, U-net: convolutional networks for biomedical image segmentation, in: N. Navab, J. Hornegger, W.M. Wells, A.F. Frangi (Eds.), Medical Image Computing and Computer-Assisted Intervention – MICCAI 2015, Springer International Publishing, Cham, 2015, pp. 234–241.
[32] E.S. Husebye, S.H. Pearce, N.P. Krone, O. Kämpe, Adrenal insufficiency, Lancet 397 (2021) 613–629.
[33] A.C. Morani, C.T. Jensen, M.A. Habra, et al., Adrenocortical hyperplasia: a review of clinical presentation and imaging, Abdom Radiol (NY) 45 (2020) 917–927.
[34] K.Y. Lam, A.C. Chan, C.Y. Lo, Morphological analysis of adrenal glands: a prospective analysis, Endocr. Pathol. 12 (2001) 33–38.
[35] A. Yiallouris, C. Tsioutis, E. Agapidaki, et al., Adrenal aging and its implications on stress responsiveness in humans, Front. Endocrinol. 10 (2019) 54.
[36] Y. Tezuka, N. Atsumi, A.R. Blinder, et al., The age-dependent changes of the human adrenal cortical zones are not congruent, J. Clin. Endocrinol. Metab. 106 (2021) 1389–1397.
[37] S. Li, H. Sun, L. Ma, et al., Left-versus-right-adrenal-volume ratio as a screening index before adrenal venous sampling to identify unilateral primary aldosteronism patients, J. Hypertens. 38 (2020) 347–353.

[38] P.J. Jenkins, S.A. Sohaib, P.J. Trainer, T.A. Lister, G.M. Besser, R. Reznek, Adrenal enlargement and failure of suppression of circulating cortisol by dexamethasone in patients with malignancy, Br. J. Cancer 80 (1999) 1815–1819.
[39] M. Biswas, J.C. Smith, J.S. Davies, Bilateral adrenal enlargement and non-suppressible hypercortisolism as a presenting feature of gastric cancer, Ann. Clin. Biochem. 41 (2004) 494–497.
[40] M.A. Alshahrani, M. Bin Saeedan, T. Alkhunaizan, I.M. Aljohani, F.M. Azzumeea, Bilateral adrenal abnormalities: imaging review of different entities, Abdom Radiol (NY) 44 (2019) 154–179.
[41] H. Nakajima, Y. Niida, E. Hamada, et al., Adrenal insufficiency in immunochemotherapy for small-cell lung cancer with ectopic ACTH syndrome, Endocrinol. Diabetes Metabol. Case Rep. (2021) 2021.
[42] B. Ludescher, A. Najib, S. Baar, et al., Increase of visceral fat and adrenal gland volume in women with depression: preliminary results of a morphometric MRI study, Int. J. Psychiatr. Med. 38 (2008) 229–240.
[43] L.V. Kessing, I.S. Willer, U. Knorr, Volume of the adrenal and pituitary glands in depression, Psychoneuroendocrinology 36 (2011) 19–27.
[44] I. Serifoglu, Oz II, M. Bilici, The adrenal gland volume measurements in manifestation of the metabolic status in type-2 diabetes mellitus patients, Internet J. Endocrinol. 2016 (2016), 7195849.
[45] S. Nougaret, B. Jung, S. Aufort, G. Chanques, S. Jaber, B. Gallix, Adrenal gland volume measurement in septic shock and control patients: a pilot study, Eur. Radiol. 20 (2010) 2348–2357.
[46] B. Jung, S. Nougaret, G. Chanques, et al., The absence of adrenal gland enlargement during septic shock predicts mortality: a computed tomography study of 239 patients, Anesthesiology 115 (2011) 334–343.
[47] N. Mongardon, G. Savary, G. Geri, et al., Prognostic value of adrenal gland volume after cardiac arrest: association of CT-scan evaluation with shock and mortality, Resuscitation 129 (2018) 135–140.
[48] S. Jin, H. Zhang, W. Pan, et al., Diagnostic value of the relative enhancement ratio of the portal venous phase to unenhanced CT in the identification of lipid-poor adrenal tumors, Abdom Radiol (NY) 47 (2022) 3308–3317.